

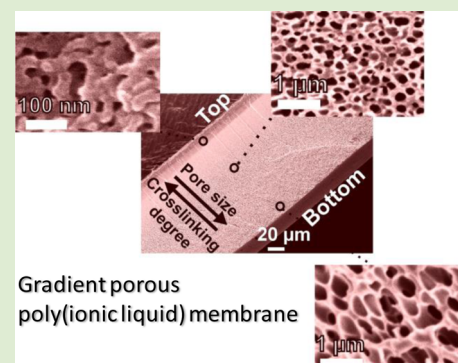
Tuning the Pore Size in Gradient Poly(ionic liquid) Membranes by Small Organic Acids

Karoline Täuber, Qiang Zhao, Markus Antonietti, and Jiayin Yuan*

Max Planck Institute of Colloids and Interfaces, Am Mühlenberg 1, 14476 Potsdam, Germany

S Supporting Information

ABSTRACT: Highly charged porous polymer membranes with adjustable pore size and gradient pore structure along the membrane cross-section were prepared by ammonia-triggered electrostatic complexation between an imidazolium-based cationic poly(ionic liquid) (PIL) and multivalent benzoic acid derivatives. The PIL and the acid compound were first dissolved homogeneously in DMSO, cast into a thin film onto a glass plate, dried, and finally immersed into an aqueous ammonia solution. The diffusion of ammonia from the top to the bottom into the film neutralized the acid and introduced the gradient pore structure and in situ electrostatic cross-linking to fix the pores. The pore size and its distribution of the membranes were found controllable in terms of the multivalency of the acids, the imidazolium/carboxylate ratio, and the nature of the PIL counteranion.



Porous polymer membranes are of significant interest in both fundamental research and industry production, with applications ranging from size selective separators, sensors, catalysts, to microelectronic devices and separators in lithium ion batteries. Many applications favorably require high levels of control over porosity, pore morphology, and pore size of the task specific membranes.^{1–4} For example, the asymmetric assembly of a top selective layer featuring small pores supported by an underlying macroporous layer represents a model structure that endows various filtration membranes with high permeability, selectivity, and robust mechanical properties.

Pores with adjustable shapes, size, and size distribution have so far been introduced into polymer membranes by several approaches.⁵ Track etching is a usual way to induce well-defined pores into a polymeric matrix via the bombardment of heavy ions, but this method is relatively expensive and inappropriate for industrial usage.⁶ Phase separation is commonly used to introduce pores of targeted size into membrane materials.^{2,7,8} Thermally induced phase separation (TIPS) and nonsolvent induced phase separation (NIPS) are two major techniques in industry to prepare porous membranes. Very recently, block copolymers emerge as popular candidates in the preparation of symmetrical and asymmetrical porous structures featuring honeycomb pores on the surface.^{9–12} However, if it comes to polyelectrolyte membranes, these approaches are not well applicable anymore because of the commonly hydrophilic and charged character of conventional polyelectrolytes.¹³ Post-treatment of nonionic porous polymers is an indirect way to obtain charged porous polymer films. Electrostatic layer by layer (LbL) assemblies of two oppositely charged polyelectrolytes on porous templates have been exploited to prepare porous polyelectrolyte membranes.^{14–16} Although very simple in its concept and

straightforward to perform, the LbL approach is mostly used for laboratory scale membrane fabrications.

We have very recently developed a facile method to fabricate free-standing hierarchical nanoporous polyelectrolyte membranes by the so-called electrostatic complexation.^{17,18} In our approach, a unique class of polyelectrolytes, poly(ionic liquid)s (PILs) that are prepared by polymerization of ionic liquid monomers, is used.^{19–26} Their favorable solubility in organic media of different polarity allows processing and construction of functional and porous polymer (nano)structures from polyelectrolytes in both organic and aqueous solvents.^{27–38} The ionic cross-linking that stabilizes the membrane pores was built up between a vinylimidazolium-based cationic PIL and neutralized multiacids, such as poly(acrylic acid) (PAA; $M_w = 2$ kDa) and pillar[5]arene derivatives with ten $-COOH$ groups. In the case of PAA as an acid source, the as-prepared membranes typically contain a thin top layer bearing irregular pores in the micrometer to submicrometer size range and a dense bottom layer with nanopores.¹⁷ When the pillar[5]arene acid was used as the acid source, homogeneous distribution of pores of $0.3–5 \mu\text{m}$ across the membrane was observed.¹⁸ So far, in spite of our rapid advance on this topic, it remained unclear to us how to effectively control the size of the pores in these PIL membranes.

We herein report a simple way of how to access polyelectrolyte membranes bearing gradient pore structure with tunable pore size by cross-linking of poly(3-cyanomethyl-1-vinylimidazolium) (PCMVIm)-based PILs with various multivalent benzoic acid derivatives. The multiacid compounds

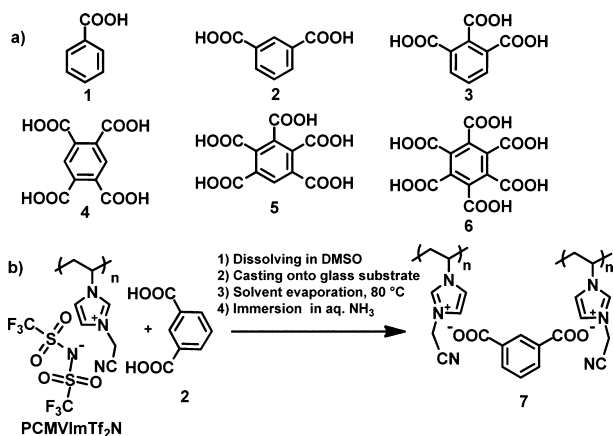
Received: October 22, 2014

Accepted: December 8, 2014

Published: December 18, 2014

employed in this study act as a model system, constructed of a benzene core and variable $-\text{COOH}$ units (acids 1–6, see Scheme 1a). In that way, the cross-linking effect on the pore size and the pore size distribution were studied systematically.

Scheme 1. (a) Chemical Structures of Different Organic Acids Used for Membrane Fabrication; (b) Fabrication Scheme of the Porous Membrane on the Example of PCMVImTf₂N with Isophthalic Acid (2)



In Scheme 1b, the fabrication procedure of the membrane is exemplified with isophthalic acid (2) and PCMVImTf₂N (Tf₂N denotes the bis(trifluoromethanesulfonyl)imide counteranion). Typically, PCMVImTf₂N and 2 were dissolved in dimethyl sulfoxide (DMSO) as polar nonprotic solvent, which keeps the acid protonated at the mixing step so that no ionic cross-linking can occur. The freshly prepared homogeneous, yellowish solution was subsequently cast onto a glass plate and the solvent was allowed to evaporate for 1 h at 80 °C. The dry polymer/acid blend film sticking firmly to the glass substrate was then immersed into an aqueous solution of ammonia (0.2 wt %), in order to allow for pore development and pore stabilization by ionic complexation. It is observed, that the transparent film turned opaque immediately when placed in aqueous ammonia solution, indicating formation of pores in submicrometer scale. The formation of the pores is triggered by the deswelling of the hydrophobic PIL as the water penetrates into the film. At the same time, neutralization of the acid by ammonia induces complexation between the cationic polymer and the in situ generated, negatively charged isophthalate, forming a densely cross-linked network to lock the pores. After 2 h, the membrane detaches easily from the glass substrate on account of its porous nature, reducing the interfacial contact with the glass plate. Fourier-transform infrared (FT-IR) spectroscopy measurements of the membrane reveal a band shift from 1679 to 1602 cm⁻¹. The former is attributed to the COO stretch of the protonated carboxylic function of isophthalic acid, and the latter is characteristic of the asymmetric COO⁻ stretch, indicating deprotonation of the acid (Figure S1). These results support the formation of an ionically cross-linked network between PCMVImTf₂N and the neutralized multivalent acid. Bearing this cross-linked network, which is known for its solvent resistance,³⁹ the membrane is stable in water, as well as in various organic solvents such as DMSO, acetone and DMF.

The membrane fabrication procedure was then applied to acids with one to six carboxylic acid units (Scheme 1). Studying

the cross sections of the as-synthesized membranes, an interesting observation was made. Unlike in our previous reports,^{17,18} the present membranes showed a profile of gradient pore structure in their cross-section (Figure 1). The

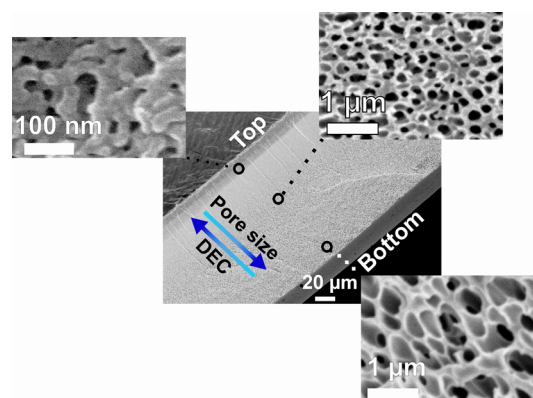


Figure 1. Cross-section of a membrane from PCMVImTf₂N and 5 in a 1:1 molar ratio.

pores were smallest in the top of the membrane (the surface in direct contact with aq. ammonia) and gradually increased in size toward the bottom (in contact with the glass plate). For a membrane built up from acid 5 and PCMVImTf₂N in a 1:1 imidazolium/carboxylate molar ratio, the pores are on average 30 nm in the top and increase to 490 nm in the bottom (Figure 1). This gradient pore structure is related to the gradual penetration of ammonia through the cross-section of the membrane, as immersion of the same film in pure water failed to produce a porous membrane.

Energy-dispersive X-ray (EDX) measurements of this membrane cross-section reveal a gradient in the concentration of sulfur from the top, where it is lowest, to the bottom of the cross-section. Sulfur, which is only present in the Tf₂N counteranion in the PIL is replaced by the carboxylate of the acid during the ionic complexation. Therefore, the sulfur content is a reliable measure of the local ionic complexation inside the membrane. An increase in the amount of sulfur from the top to the bottom is characteristic for a drop in the degree of electrostatic complexation (DEC; see Supporting Information), which denotes the relative portion of the imidazolium units along the PIL chain that join the cross-linked network. The DEC gradient has also been observed in our previous systems; however it has not resulted in a gradient pore structure, but either a hierarchical two-zone or a uniform pore structure formed. As we know, in the immersion step of the film into aqueous ammonia solution, two processes start, that is, the neutralization of the multiacids that induces the cross-linking with PILs, and the parallel water diffusion that deswells the hydrophobic PIL to construct the pores. We assume that the present gradient in the pore size is linked to the higher acidity of the benzoic acid derivatives compared with PAA and the pillar[5]arene acids. Hence, ionic cross-linking, which is triggered by the acid–base neutralization is faster, especially in the upper regions of the membrane, where the concentration of ammonia is the highest. Therefore, the accelerated cross-linking reaction stabilizes the pores at their early period before they grow larger. As the concentration of ammonia decreases toward the bottom, deswelling of the polymer is more pronounced than in the upper parts and as a consequence, a gradient pore structure forms.

The pore structure of the membrane as a function of the multivalency of the organic acids was then studied in detail for membranes prepared from acids 2–6. The average pore size (average of the whole cross-section) of the membranes decreases in general with an increase in the COOH number on the benzoic acids (Figure 2, Table S1). The pores of the

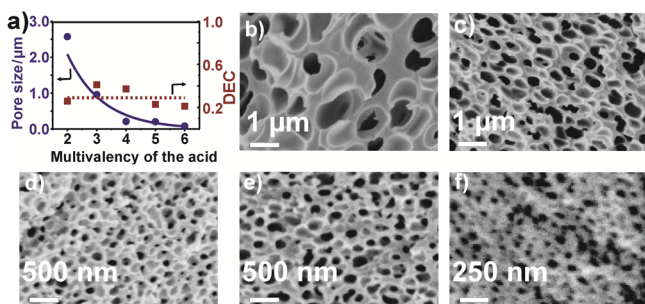


Figure 2. (a) Plots of the pore size of PCMVImTf₂N membrane cross sections and DEC vs the multivalency of the benzoic acids used for cross-linking. The dashed line refers to the mean value of DEC. (b–f) SEM images of the cross sections of the membranes prepared from PCMVImTf₂N and acid: (b) 2, (c) 3, (d) 4, (e) 5, and (f) 6.

membranes are the largest, 2.6 μm in average, for the system containing diacid 2 (Figure 2b). As increasing the number of acid functions on the benzoic acid decreases the pore size (Figure 2c–e), the pores were the smallest for the membrane from hexavalent acid 6, only 80 nm in average (Figure 2f). No membrane was obtained from the monoacid 1 as lack of ionic cross-linking and stable network.

Studying the overall DEC of the membranes by elemental analysis of sulfur, it was found that the DEC value is similar to each other for membranes from acids 2–6, around 30 ± 10% (dashed line, Figure 2a). This is well explained by the fact that the imidazolium/COOH molar ratio was kept at 1 for all the samples. However, the acid compounds bearing more –COOH groups form denser cross-linked networks, that is, build up a higher cross-linking density, which denotes a higher number of ionically cross-linked joints per volume unit. A more densely cross-linked network is more likely to stabilize smaller pores, as a higher mechanical strength must exist against the capillary force that is stronger for smaller pores.

The dependence of the pore size on the DEC has been studied by changing the imidazolium/COOH molar ratio for membranes from PCMVImTf₂N and acids 2, 3, and 4 (Figure 3). The general observed tendency was that the average pore size of the membranes is larger at a higher imidazolium/COOH molar ratio. Taking for illustration the system composed of acid 3 and PCMVImTf₂N: When the COOH/imidazolium molar amount is 3, a maximum DEC of 98% was reached and the

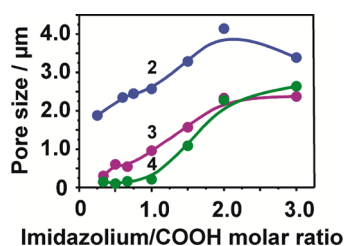


Figure 3. (a) Averaged pore size as a function of the relative molar amount of PCMVImTf₂N and acid 2, 3, and 4.

averaged pore size is the smallest (300 nm in average) for this system. By increasing the amount of imidazolium units, the DEC gradually decreased to 13% and the pore size went up to 2.3 μm at an imidazolium/COOH ~ 3. Similar results were found for membranes from acids 2 and 3. However, the curve for acid 2 differs slightly from the other two, as the pore size decreases unexpectedly after having reached a maximum of 4.1 μm at an imidazolium/COOH ~ 2. To our opinion, the incorporation of excessive PILs into the system enhances the mobility of polymer chains due to the low DEC and cross-linking density. The polymer chains may therefore stretch into the pores to decrease the pore size. These results show that porous polyelectrolyte membranes with gradient and tunable pore size in a broad range can be obtained from a single multivalent acid and a cationic PIL, by simply varying the DEC of the system.

The pore size of the membrane has furthermore been studied in dependence of the counteranion type of the PIL. The hypothesis of pore formation by deswelling of the hydrophobic PIL in contact with water was confirmed by our experiments, where hydrophilic PIL, PCMVImBr with acid 2 yielded nonporous membranes, proven by SEM and gas sorption measurement (see Supporting Information for N₂ isotherms and SEM images), whereas the pores from hydrophobic PCMVImPF₆ and PCMVImBF₄ were in the micrometer range (Figure S4). Summarizing these results, the pore sizes were in the order of Br ≪ Tf₂N < PF₆ < BF₄ (Table 1, Figure

Table 1. Average Pore Sizes of Membranes Prepared from Acid 2 and PCMVIm with Different Counteranions

PCMVImX (X =)	pore size (μm)
Br	–
Tf ₂ N	1.2
PF ₆	1.4
BF ₄	2.5

S3). These results highlight that besides the acid choice and the imidazolium/COOH ratio, hydrophobicity of the PIL also plays a role in the formation of the pores in the membrane.

In conclusion, we have presented our recent process of how to access porous polyelectrolyte membranes with a gradient in both cross-linking density and pore size along the cross-section via the usage of a poly(ionic liquid). The pore sizes and pore size gradient of the membranes have been effectively tuned by the choice of benzoic acid derivatives with different multivalency, the variation of the imidazolium/COOH molar ratio, and the type of the PIL counteranion. Having these parameters in hand, one can push forward the fabrication technique of nanoporous asymmetric poly(ionic liquid) membranes with a high level of complexity and function yet via an easy-to-perform synthetic protocol.

■ ASSOCIATED CONTENT

📄 Supporting Information

Experimental procedures and further pore size data, FTIR and N₂ sorption measurement results, and calculation of DEC. This material is available free of charge via the Internet at <http://pubs.acs.org>.

■ AUTHOR INFORMATION

Corresponding Author

*E-mail: jiayin.yuan@mpikg.mpg.de.

Notes

The authors declare no competing financial interest.

ACKNOWLEDGMENTS

The authors thank the Max-Planck society for financial support. Marc Ledendecker is acknowledged for help with the EDX measurements.

REFERENCES

- (1) van Rijn, P.; Tutus, M.; Kathrein, C.; Zhu, L.; Wessling, M.; Schwaneberg, U.; Boker, A. *Chem. Soc. Rev.* **2013**, *42* (16), 6578–6592.
- (2) Stein, A. *Adv. Mater.* **2003**, *15* (10), 763–775.
- (3) Warkiani, M. E.; Bhagat, A. A. S.; Khoo, B. L.; Han, J.; Lim, C. T.; Gong, H. Q.; Fane, A. G. *ACS Nano* **2013**, *7* (3), 1882–1904.
- (4) Wan, L.-S.; Zhu, L.-W.; Ou, Y.; Xu, Z.-K. *Chem. Commun. (Cambridge, U. K.)* **2014**, *50* (31), 4024–4039.
- (5) Lalia, B. S.; Kochkodan, V.; Hashaikeh, R.; Hilal, N. *Desalination* **2013**, *326* (0), 77–95.
- (6) Apel, P. *Radiat. Meas.* **2001**, *34* (1–6), 559–566.
- (7) Nunes, S. P.; Car, A. *Ind. Eng. Chem. Res.* **2012**, *52* (3), 993–1003.
- (8) Schulze, M. W.; McIntosh, L. D.; Hillmyer, M. A.; Lodge, T. P. *Nano Lett.* **2013**, *14* (1), 122–126.
- (9) Ulbricht, M. *Polymer* **2006**, *47* (7), 2217–2262.
- (10) Peinemann, K.-V.; Abetz, V.; Simon, P. F. W. *Nat. Mater.* **2007**, *6* (12), 992–996.
- (11) Takekoh, R.; Russell, T. P. *Adv. Funct. Mater.* **2014**, *24* (10), 1483–1489.
- (12) Xu, T.; Zhao, N.; Ren, F.; Hourani, R.; Lee, M. T.; Shu, J. Y.; Mao, S.; Helms, B. A. *ACS Nano* **2011**, *5* (2), 1376–1384.
- (13) Tokarev, I.; Orlov, M.; Minko, S. *Adv. Mater. (Weinheim, Ger.)* **2006**, *18* (18), 2458–2460.
- (14) Lutkenhaus, J. L.; McEnnis, K.; Hammond, P. T. *Macromolecules* **2008**, *41* (16), 6047–6054.
- (15) Hiller, J. A.; Mendelsohn, J. D.; Rubner, M. F. *Nat. Mater.* **2002**, *1* (1), 59–63.
- (16) Li, Q.; Quinn, J. F.; Caruso, F. *Adv. Mater. (Weinheim, Ger.)* **2005**, *17* (17), 2058–2062.
- (17) Zhao, Q.; Yin, M.; Zhang, A. P.; Prescher, S.; Antonietti, M.; Yuan, J. *J. Am. Chem. Soc.* **2013**, *135* (15), 5549–5552.
- (18) Zhao, Q.; Dunlop, J. W. C.; Qiu, X.; Huang, F.; Zhang, Z.; Heyda, J.; Dzubiella, J.; Antonietti, M.; Yuan, J. *Nat. Commun.* **2014**, *5*.
- (19) Green, O.; Grubjesic, S.; Lee, S.; Firestone, M. A. *Polym. Rev. (Philadelphia, PA, U. S.)* **2009**, *49* (4), 339–360.
- (20) Kuzmicz, D.; Coupillaud, P.; Men, Y.; Vignolle, J.; Vendraminotto, G.; Ambrogio, M.; Taton, D.; Yuan, J. *Polymer* **2014**, *55* (16), 3423–3430.
- (21) Bandomir, J.; Schulz, A.; Taguchi, S.; Schmitt, L.; Ohno, H.; Sternberg, K.; Schmitz, K.-P.; Kragl, U. *Macromol. Chem. Phys.* **2014**, *215* (8), 716–724.
- (22) Coupillaud, P.; Fèvre, M.; Wirotius, A.-L.; Aissou, K.; Fleury, G.; Debuigne, A.; Detrembleur, C.; Mecerreyes, D.; Vignolle, J.; Taton, D. *Macromol. Rapid Commun.* **2014**, *35* (4), 422–430.
- (23) He, H.; Zhong, M.; Luebke, D.; Nulwala, H.; Matyjaszewski, K. *J. Polym. Sci., Part A: Polym. Chem.* **2014**, *52* (15), 2175–2184.
- (24) He, H.; Averick, S.; Roth, E.; Luebke, D.; Nulwala, H.; Matyjaszewski, K. *Polymer* **2014**, *55* (16), 3330–3338.
- (25) Shaplov, A. S.; Vlasov, P. S.; Armand, M.; Lozinskaya, E. I.; Ponkratov, D. O.; Malyshkina, I. A.; Vidal, F.; Okatova, O. V.; Pavlov, G. M.; Wandrey, C.; Godovikov, I. A.; Vygodskii, Y. S. *Polym. Chem.* **2011**, *2* (11), 2609–2618.
- (26) Zhao, Q.; Soll, S.; Antonietti, M.; Yuan, J. *Polym. Chem.* **2013**, *4* (8), 2432–2435.
- (27) Choi, J.-H.; Ye, Y.; Elabd, Y. A.; Winey, K. I. *Macromolecules* **2013**, *46* (13), 5290–5300.
- (28) Jangu, C.; Wang, J.-H. H.; Wang, D.; Sharick, S.; Heflin, J. R.; Winey, K. I.; Colby, R. H.; Long, T. E. *Macromol. Chem. Phys.* **2014**, *215* (13), 1319–1331.
- (29) Nguyen, P. T.; Wiesenauer, E. F.; Gin, D. L.; Noble, R. D. *J. Membr. Sci.* **2013**, *430* (0), 312–320.
- (30) Lu, J.; Yan, F.; Texter, J. *Prog. Polym. Sci.* **2009**, *34* (5), 431–448.
- (31) Mecerreyes, D. *Prog. Polym. Sci.* **2011**, *36* (12), 1629–1648.
- (32) England, D.; Tambe, N.; Texter, J. *ACS Macro Lett.* **2012**, *1* (2), 310–314.
- (33) Yan, F.; Texter, J. *Angew. Chem., Int. Ed.* **2007**, *46* (14), 2440–2443.
- (34) Texter, J. *Curr. Opin. Colloid Interface Sci.* **2014**, *19* (2), 43–48.
- (35) England, D.; Yan, F.; Texter, J. *Langmuir* **2013**, *29* (38), 12013–12024.
- (36) Wiesenauer, E. F.; Nguyen, P. T.; Newell, B. S.; Bailey, T. S.; Noble, R. D.; Gin, D. L. *Soft Matter* **2013**, *9* (33), 7923–7927.
- (37) McDanel, W. M.; Cowan, M. G.; Carlisle, T. K.; Swanson, A. K.; Noble, R. D.; Gin, D. L. *Polymer* **2014**, *55* (16), 3305–3313.
- (38) Chu, F.; Lin, B.; Yan, F.; Qiu, L.; Lu, J. *J. Power Sources* **2011**, *196* (19), 7979–7984.
- (39) Zhao, Q.; An, Q.; Ji, Y. L.; Qian, J. W.; C-J, G. *J. Membr. Sci.* **2011**, *379*, 19–45.